The Kärger vs bi-exponential model: theoretical insights and experimental validations

Nicolas Moutal, Markus Nilsson, Daniel Topgaard, Denis S Grebenkov

The Kärger vs bi-exponential model: theoretical insights and experimental validations

Nicolas Moutal[a], Markus Nilsson[b], Daniel Topgaard[b], Denis Grebenkov[a,*]

[a] *PMC, CNRS Ecole Polytechnique, F-91128, Palaiseau, France*
[b] *Physical Chemistry, Lund University, P.O.B. 124, SE-22100 Lund, Sweden*

A B S T R A C T

We revise three common models accounting for water exchange in pulsed-gradient spin-echo measurements: a bi-exponential model with time-dependent water fractions, the Kärger model, and a modified Kärger model designed for restricted diffusion, e.g. inside cells. The three models are compared and applied to experimental data from yeast cell suspensions. The Kärger model and the modified Kärger model yield very close results and accurately fit the data. The bi-exponential model, although less rigorous, has a natural physical interpretation and suggests a new experimental modality to estimate the water exchange time.

1. Introduction

Diffusion Magnetic Resonance Imaging (dMRI) is a non-invasive technique allowing one to probe diffusion of nuclei in complex systems, in particular biological samples, with strong medical applications to brain and lung imaging [1–6]. In the case of free diffusion in a homogeneous medium, the classical Stejskal-Tanner formula for pulsed-gradient spin-echo (PGSE) sequences yields the signal $S = S_0 \exp(-bD)$, where S_0 is the reference signal, D is the diffusion coefficient of the spin-bearing particles in the medium and $b = \gamma^2 g^2 \delta^2 t_d$, where γ is the nuclear gyromagnetic ratio, g the magnetic field gradient, δ the gradient pulse duration and $t_d = \Delta - \delta/3$ (Δ being the delay between the two gradient pulses) [7]. In biological systems, however, the restriction of diffusion by membranes or obstacles leads to a more complex dependence of the signal on the experimental variables g, δ, t_d [3, 8]. A common strategy to fit non-exponential signal and to interpret the measurements consists in splitting the signal into two contributions: one coming from hindered diffusion in the extracellular space and the other from restricted diffusion in the intracellular space. The signal is thus fitted by a bi-exponential model, which yields the "fast" and "slow" apparent diffusion coefficients (ADC), respectively [9–14].

The bi-exponential model is a convenient fit but its interpretations are not always correct [15]. The distinction between free water and restricted water may be artificial [12, 16, 17]. Moreover, the slow apparent diffusion coefficient often depends on the parameters of the gradient sequence, for example, the pulse duration δ, that makes any comparison (and interpretation) between different experiments difficult or even impossible [10, 11]. Finally, exchange of water between the intracellular and extracellular compartments may affect the result of the fit [18, 19]. It is worth stressing that the bi-exponential function is very flexible and allows to fit accurately a generic decaying signal. However, a good fit is not a definite "proof" of the underlying hypotheses of the model [15, 20].

In order to account for exchange between the two pools of water, Kärger introduced in [21, 22] a model that was then developed to study diffusion NMR signals and is in some sense an extension of the bi-exponential model [23–26]. The main idea consists in characterizing diffusion in the complex structure of the medium by macroscopic quantities, namely diffusion coefficients and exchange times. Fieremans *et al* showed by Monte Carlo simulations that such a coarse-graining approach is valid in the regime of small cells and long exchange times. More explicitly, one has the conditions

$$\sqrt{Dt} \gg l_c\,, \qquad \text{and} \qquad \sqrt{D\tau} \gg l_c\,, \tag{1}$$

namely, the diffusion length $\sqrt{Dt}$ should be much larger than the correlation length of the medium l_c and, at

*Corresponding author: Tel: +33 1 69 33 47 39
e-mail: nicolas.moutal@polytechnique.edu (Nicolas Moutal), denis.grebenkov@polytechnique.edu (Denis Grebenkov)

the same time, the exchange time τ should be much longer than the exploration time ${l_c}^2/D$ ("barrier-limited exchange") [27, 28]. This allows one to treat any complex medium as a "homogeneous" one where the exchange takes place at every point in space, which is the fundamental hypothesis of the Kärger model.

The Kärger model originally relied on the narrow-pulse approximation (NPA) which is typically non valid for restricted diffusion inside compartments of a few microns if the encoding duration δ is greater than a few milliseconds. In [29, 30] the Kärger model was rigorously extended to finite pulses, but the resulting ordinary differential equations need to be solved numerically. A "modified" Kärger model in which the slow ADC is set to zero was also proposed in order to account for restricted diffusion [31]. Note that the derivation in [29, 30] yields the same modified Kärger model with zero intracellular ADC, see Eqs. (20-29) from Ref. [30].

In this article, we critically revise the derivation of these three models (bi-exponential, Kärger model and modified Kärger model) and then apply them to analyze pulsed-gradient stimulated spin-echo experiments with yeast cells. The Kärger model and the modified Kärger model are shown to be very close to each other in the relevant range of parameters, whereas the bi-exponential model exhibits some deviations at low gradients. All three models fit the data well and give access to the exchange time across the cell membranes.

2. Models

For the sake of clarity and being motivated by experiments with yeast cells, we consider a medium that contains spherical cells of radius R. The diffusion coefficient of extracellular water is denoted by D_e whereas the diffusion coefficient of intracellular water is denoted by D_i. We stress that these are the "true" diffusion coefficients and not ADCs extracted from spin-echo signals. In the following we implicitly assume that the spin-echo signals are normalized by the reference signal at zero gradient, i.e. $S(g = 0) = 1$.

Under the Gaussian phase approximation (GPA) and in the absence of exchange, Neuman derived the decay of the intracellular signal S_i [32]:

$$S_i \simeq \rho \exp(-D_s b) \,, \tag{2}$$

$$D_s = \frac{4R^2}{\xi t_d} \sum_{n=1}^{\infty} \frac{1 - \frac{1}{{\alpha_n}^2 \xi} F_n(\xi, \Delta/\delta)}{{\alpha_n}^4 ({\alpha_n}^2 - 2)} \,, \tag{3}$$

$$F_n(\xi, \Delta/\delta) = 1 - e^{-{\alpha_n}^2 \xi} + 2e^{-{\alpha_n}^2 \xi \Delta/\delta} \sinh^2({\alpha_n}^2 \xi/2) \,,$$

where ρ is the intracellular water volume fraction, $\xi = D_i \delta / R^2$ and α_n are the zeroes of the derivative of the spherical Bessel function j_1: $\alpha_1 \approx 2.08, \alpha_2 \approx 5.94, \ldots$. The coefficient D_s is thus the apparent "slow" diffusion coefficient probed by NMR. However, it is important to note that D_s cannot be interpreted as a measure of mean-squared displacement since it depends *a priori* on δ. When ${\alpha_1}^2 \xi \gtrsim 1$ one can rewrite Eq. (3) with a very good approximation as:

$$D_s \approx \frac{16R^2}{175 \xi t_d} \left(1 - \frac{F_1(\xi, \Delta/\delta)}{{\alpha_1}^2 \xi}\right) . \tag{4}$$

In the limit $\xi \to \infty$ one recovers the well-known motional narrowing formula [3]:

$$D_s \underset{\xi \gg 1}{\approx} \frac{16R^4}{175 D_i \delta t_d} \,. \tag{5}$$

Unlike Eqs. (2) and (3) which require $qR \ll 2\pi$, with $q = \gamma g \delta$, in order to satisfy the GPA, one can use Eq. (2) with Eq. (5) under the much weaker condition $qR \ll \xi$. In contrast, when this condition is not satisfied (i.e. $qR \gg \xi \gg 1$), the GPA fails, and the signal exhibits "abnormal" dependence on the b-value, such as $-log(S) \sim b^{1/3}$ in the localization regime [33–37].

However, in typical experiments, $D_i \sim 1\ \mu\text{m}^2/\text{ms}$, $\delta \sim 1 - 10$ ms and $R \sim 1 - 5\ \mu$m which makes the condition $\xi \gg 1$ difficult to achieve. Therefore one generally has to carefully check the validity of the GPA, especially for the small values of ξ (i.e., δ).

In the absence of exchange across cell membranes, the complete signal can then be written as:

$$S = (1 - \rho) \exp\Big(-D_f b\Big) + \rho \exp(-D_s b) \,, \tag{6}$$

where D_f is the apparent "fast" diffusion coefficient, which is smaller than the intrinsic D_e because the extracellular diffusion is hindered by the cells. Moreover, D_f may decrease slowly with t_d as demonstrated in [38–40]. Note that this involves already an approximation because we reduce the complex problem of diffusion in the extracellular medium to an apparent diffusion coefficient, ignoring for example localization effects at the cell boundaries [34–36, 41]. Now we investigate the effect of exchange accounted via three models.

2.1. Bi-exponential model with time-dependent water fractions

The most simple idea is to keep Eq. (6) but to consider time-dependent intracellular water fraction ρ.

Let us think of the magnetic field encoded water inside one cell as a "marked" water, which has intracellular and extracellular concentrations c_i and c_e, respectively (at the beginning, $c_e = 0$). This relies on the assumption that δ is sufficiently short so that water molecules stay inside the cell during the encoding. We also assume that the

leakage is slow so that the intracellular concentration c_i is at all times homogeneous inside the cell ("pore equilibration" [42]). Finally, we neglect the re-entrance of water because of the dilution in the extracellular medium: $c_e \ll c_i$. Then during the diffusion time the net rate of leakage of this marked water is $\kappa A c_i$, where κ is the permeability of the cell membrane and A its area, which yields the differential equation

$$\frac{\mathrm{d}c_i}{\mathrm{d}t} = -\frac{\kappa A c_i}{V} \,, \tag{7}$$

where V is the volume of the cell, from which one gets the classic formula

$$c_i = c_i^0 \exp(-t/\tau_{i\to e}) \,, \quad \tau_{i\to e} = \frac{V}{A\kappa} \,. \tag{8}$$

For a sphere of radius R the expression of $\tau_{i\to e}$ can be simplified (and for an arbitrary shape of diameter $2R$ the result is always smaller):

$$\tau_{i\to e} = \frac{R}{3\kappa} \,. \tag{9}$$

We can now come back to our assumptions: (i) the encoding is sufficiently short to neglect the effect of permeability, i.e. $\delta \ll \tau_{i\to e}$; (ii) the intracellular medium is homogeneous at all times, i.e. $\tau_{i\to e} \gg R^2/D_i$ or $R \ll D_i/\kappa$. One recognizes on the right-hand side the "permeability length" which represents the typical distance traveled by a particle near a boundary before crossing it [43–46]. As we are in the restricted diffusion regime $\delta \gtrsim R^2/D_i$ we only have to check the first hypothesis. Note that this corresponds to the conditions of applicability of the Kärger model (1), with $l_c = R$.

The above reasoning can be extended to multiple cells. In this case one still considers the intracellular water as marked water, but with individual markings for each cell. Indeed, Eqs. (2) and (3) are valid only for water that stays inside the same cell. The magnetization of water molecules that travels from cell to cell is destroyed in the same way as freely diffusing water (actually, this is only true if the cells are not regularly arranged on a lattice, that we implicitly assume here).

The above analysis implies that ρ should decay with t_d according to Eq. (8):

$$\rho = \rho_0 \exp(-t_d/\tau_{i\to e}) \,. \tag{10}$$

This model is *a priori* only applicable in the case when the extracellular diffusion rapidly destroys the magnetization, that is $q^2 D_f \tau_{i\to e} \gg 1$. Indeed, otherwise one should also take into account the entry of extracellular water whose magnetization is not negligible.

2.2. Kärger Model

The classical model for treating exchange between two compartments with different diffusion coefficients is the Kärger model [23, 24]. Roughly speaking, this is an extension of the bi-exponential model with an additional parameter: an exchange time τ_K which is the time-scale of the leakage from one compartment to the other. More precisely,

$$\tau_{i\to e} = \rho\tau_K \qquad \text{and} \qquad \tau_{e\to i} = (1-\rho)\tau_K \tag{11}$$

are respectively the mean times for crossing the membranes from the inside to the outside and from the outside to the inside. The Kärger model relies on the assumption that $\delta \ll \tau_K$, which allows one to neglect the effect of exchange during the encoding and decoding gradient pulses. This means that, as far as the exchange is concerned, one can use $t_d = \Delta - \delta/3$ instead of, say, $\Delta + \delta$, as the total time during which the exchange takes place. As a matter of fact, in the case of long-exchange times, it was shown that using this form of t_d as the total time improves the accuracy of the Kärger model to the first order in δ/Δ [47, 48]. In addition, it makes the comparison with the bi-exponential model easier.

Solving the system of differential equations on the intra- and extracellular signals

$$\begin{cases} \dfrac{\mathrm{d}S_i}{\mathrm{d}t} = -D_s q^2 S_i - S_i/\tau_{i\to e} + S_e/\tau_{e\to i} & \text{(12a)} \\[2ex] \dfrac{\mathrm{d}S_e}{\mathrm{d}t} = -D_f q^2 S_e - S_e/\tau_{e\to i} + S_i/\tau_{i\to e} & \text{(12b)} \end{cases}$$

and the initial conditions

$$S_i(t=0) = \rho \,, \quad S_e(t=0) = 1-\rho \,, \tag{13}$$

one gets the Kärger formula

$$S = P_1 \exp\!\left(-D_1 q^2 t_d\right) + P_2 \exp\!\left(-D_2 q^2 t_d\right) , \tag{14}$$

where P_1, P_2, D_1, D_2 are functions of q given by

$$\begin{aligned} D_{1,2} &= \frac{1}{2}\left(X_e + X_i \mp \sqrt{(X_e - X_i)^2 + \frac{4}{q^4 \tau_{e\to i}\tau_{i\to e}}} \right) , \\ X_e &= D_f + \frac{1}{q^2\tau_{e\to i}} \,, \qquad X_i = D_s + \frac{1}{q^2\tau_{i\to e}} \,, \\ P_1 &= \frac{D_2 - \rho D_s - (1-\rho)D_f}{D_2 - D_1} \,, \\ P_2 &= \frac{\rho D_s + (1-\rho)D_f - D_1}{D_2 - D_1} \,. \end{aligned}$$

Note that some authors [31, 49] claim using 4 initial conditions for the two first-order differential equations (12a) and (12b) even though only 2 conditions are

needed. In our notations, the two additional conditions are

$$\left.\frac{\mathrm{d}S_i}{\mathrm{d}t}\right|_{t=0} = -D_s q^2 \rho \ , \quad \left.\frac{\mathrm{d}S_e}{\mathrm{d}t}\right|_{t=0} = -D_f q^2 (1-\rho) \ , \quad (15)$$

which are actually equivalent to each other and compatible with Eq. (11). Although one can interpret these redundant initial conditions as another way to state Eq. (11), it is more natural, from the mathematical point of view, to discard Eq. (15), keeping the two initial conditions (13) and two physical relations (11).

2.3. Modified Kärger model

One obvious flaw of the Kärger model is that D_s, which was supposed to be a constant intrinsic diffusion coefficient, depends on the diffusion time (see Eq. (4)). Although it seems to be of no consequence in the final formula (14), it is a serious issue when one looks at the original equation (12a). Should one treat D_s first as a constant and then add its time dependence in the final formula or on the contrary consider that it is time-dependent from the beginning? Another defect is that the Kärger model is not supposed to be valid in the restricted diffusion regime $\xi \gtrsim 1$. In this case, the equation for the intracellular signal should be modified.

Actually, if one goes back to Eq. (2), one can see that the time-dependence of D_s in Eq. (4) is simply another way to state that the intracellular signal does not depend on the diffusion time in the restricted diffusion regime. Thus one can modify the Kärger model in the following way, inspired by [31]:

$$\begin{cases} \dfrac{\mathrm{d}S_i}{\mathrm{d}t} = -S_i/\tau_{i\to e} + S_e/\tau_{e\to i} & (16a) \\ \dfrac{\mathrm{d}S_e}{\mathrm{d}t} = -D_f q^2 S_e - S_e/\tau_{e\to i} + S_i/\tau_{i\to e} & (16b) \end{cases}$$

with the initial conditions

$$S_i(t=0) = \alpha\rho \quad S_e(t=0) = 1-\rho \ , \quad (17)$$

where $\alpha = \exp(-D_s b) < 1$ depends on q and δ but not on t_d. Compared to the Kärger model, the intracellular ADC is set to zero and the initial condition for the intracellular signal is different. Here, α is the time-independent decrease of the intracellular signal computed by Neuman formulas (2) and (3). One can see that Eqs. (16a) and (16b) provide the correct solution in the absence of exchange ($\tau_{i\to e}, \tau_{e\to i} \to \infty$).

The main physical motivation behind this model is that the intracellular magnetization reaches an equilibrium on a much shorter time-scale than the water exchange through the cell membranes ($R^2/D_i \ll \tau_K$). Because it does not evolve after this very short transient regime (in the absence of exchange), the corresponding ADC is set to zero. The initial value $\alpha\rho$ that we set for the intracellular signal is precisely the value of the signal resulting from this transient regime.

Solving Eqs. (16a) and (16b) yields

$$S = P'_1 \exp\left(-D'_1 q^2 t_d\right) + P'_2 \exp\left(-D'_2 q^2 t_d\right) , \quad (18)$$

where P'_1, P'_2, D'_1, D'_2 are functions of q given by

$$D'_{1,2} = \frac{1}{2}\left(X'_e + X'_i \mp \sqrt{(X'_e - X'_i)^2 + \frac{4}{q^4 \tau_{e\to i}\tau_{i\to e}}} \right) ,$$
$$X'_e = D_f + \frac{1}{q^2\tau_{e\to i}} \ , \qquad X'_i = \frac{1}{q^2\tau_{i\to e}} \ ,$$
$$P'_1 = \frac{D_2(1-\rho(1-\alpha)) - (1-\rho)D_f}{D_2 - D_1} \ ,$$
$$P'_2 = \frac{(1-\rho)D_f - D_1(1-\rho(1-\alpha))}{D_2 - D_1} \ .$$

One can see that the formulas for D'_1 and D'_2 are the same as the ones from the Kärger model with D_s set to zero. However, the formulas for P'_1 and P'_2 are different due to the change of initial conditions.

As in the previous section, we note that some authors [31, 49] write 4 initial conditions instead of 2 for Eqs. (16a) and (16b). Their two additional conditions read in our notations as

$$\left.\frac{\mathrm{d}S_i}{\mathrm{d}t}\right|_{t=0} = 0 \ , \quad \left.\frac{\mathrm{d}S_e}{\mathrm{d}t}\right|_{t=0} = -D_f q^2 (1-\rho) \ , \quad (19)$$

which are equivalent to each other but *not* compatible with Eq. (11). Because these authors probably used the same initial conditions (17) as us for the derivations, their formulas are the same as ours. However, the additional conditions (19) implicitly discard Eq. (11), which expresses the conservation of mass and is thus a fundamental relationship between exchange times and water fractions. To avoid further confusion, the incompatible conditions (19) should be discarded.

2.4. Comparison of the models

We have considered three different macroscopic models for the exchange between the intracellular and the extracellular water in the restricted diffusion regime. The bi-exponential model is the most simple and intuitive one, the Kärger model is the canonical one, whereas the modified Kärger model is the most rigorous of the three in this situation. It seems natural to ask whether these three models give similar or different results and under which conditions.

First, it follows from the mathematical definition of the modified Kärger model that it coincides with the Kärger model in the limit $D_s/D_f \to 0$. However, from a

physical point of view, the modified Kärger model makes sense only if D_s is inversely proportional to t_d, which necessarily implies that $D_s \ll D_i$ (see Eq. (4)) and thus $D_s \ll D_f$. As a consequence, when the Kärger model and the modified Kärger model are applicable, they generally yield results that are close to each other.

As for the bi-exponential model with decreasing fraction ρ, one can expand the Kärger model at high gradients and long exchange time ($D_f q^2 \tau_K \gg 1$) to get:

$$D_1 \approx D_s + \frac{1}{q^2 \tau_{i\to e}} , \tag{20a}$$

$$D_2 \approx D_f , \tag{20b}$$

$$P_1 \approx \rho , \tag{20c}$$

$$P_2 \approx (1-\rho) , \tag{20d}$$

that shows that the bi-exponential model is close to the Kärger model in this regime. To see this, we treat separately the cases of short and long diffusion times. At short times ($D_f q^2 t_d \lesssim 1$), the extracellular signal is not completely attenuated, but one has $t_d \lesssim (D_f q^2)^{-1} \ll \tau_K$ so that exchange can be neglected. In other words, one can use $D_1 \approx D_s$ and $D_2 \approx D_f$, which yields the standard bi-exponential model. At long times ($D_f q^2 t_d \gg 1$), the extracellular signal is completely attenuated, and the total signal reduces to the intracellular part:

$$P_1 \exp\Big(-D_1 q^2 t_d\Big) \approx \rho \exp\Big(-D_s q^2 t_d\Big) \exp\left(-\frac{t_d}{\tau_{i\to e}}\right) , \tag{21}$$

which again coincides with the bi-exponential model with variable water fractions. Discrepancies between the two models appear at low gradients ($D_f q^2 \tau_K \ll 1$), which is consistent with the remark at the end of Sec. 2.1.

In the next section we apply these three models to experimental data on yeast cells to compare their quality and range of applicability.

3. Material and Methods

Baker's yeast (Jästbolaget, Sweden) was purchased at a local supermarket, diluted with tap water in approximate volume ratio 1:2 (yeast:water), transferred to a 5 mm NMR tube, stored in room temperature for four days, and finally centrifuged at 1500g for 2 min to form a packed cell sediment of 2 cm height. NMR experiments were performed on a Bruker Avance-II spectrometer operating at 500.13 MHz ^{1}H resonance frequency. The magnet was fitted with a Bruker MIC-5 probe with 3 T/m maximum gradient at a current of 60 A. The ^{1}H signal of water was recorded with a pulsed gradient stimulated echo sequence [50] for an array of values of q, δ, and t_d [51–53]. More precisely, four values of δ were used: 3.0 ms, 5.6 ms, 10.6 ms, 20 ms, and six values for $t_d = \Delta - \delta/3$: 20.2 ms, 35.2 ms, 187.2 ms, 327.2 ms, 572.1 ms, 1000.2 ms, yielding 24 different curves. To avoid spurious effects of differences in T_2 between the intra- and extracellular components [54], the time duration for transverse relaxation was held constant at 44.8 ms for all measurements.

The variable $q = \gamma g \delta$ took 26 logarithmically spaced values from $5.3 \cdot 10^{-3}$ μm^{-1} to 1.4 μm^{-1} whatever δ and t_d. The parameter $b = q^2 t_d$ reached maximum values of about 40 ms/μm^2 for $t_d = 20.2$ ms and about 2000 ms/μm^2 for $t_d = 1000$ ms. The signal was systematically renormalized by the value S_0 at $b = 0$ obtained by fitting a single exponential function $S = S_0 \exp(-bD)$ to data points fulfilling $S/S_0 > 0.8$. Before performing any fit, we determined the noise level of the data to be about 0.25%. Because the signal never goes down below $3 \cdot 10^{-2}$ we conclude that the signal-to-noise ratio is always bigger than 10.

4. Results

The typical radius of the yeast cells is 2.5 μm. The smallest encoding duration δ is 3 ms for which $(D_i \delta)^{1/2} \sim 2\,\mu$m, implying the restricted diffusion regime ($\xi \approx 1$), but not the motional narrowing regime ($\xi \to \infty$). The advantage of being in this intermediate regime is that by fitting D_s with Eq. (4), one can estimate the two physical quantities R and D_i, that is not possible in the motional narrowing regime (cf. Eq. (5)) [55].

4.1. Bi-exponential model with decaying ρ

We have applied the fit (6) to all the values of δ and t_d. The quality of the fit was assessed by the value of the residual error, which was very close to the estimated noise value, indicating a good fit. Moreover, the 95% confidence intervals on the fit parameters were each time about: $\rho \pm 1\%$, $D_f \pm 2\%$, $D_s \pm 4\%$.

The intracellular water fraction ρ does not depend on δ and decreases with t_d, from 0.42 at $t_d = 20.2$ ms to 0.23 at $t_d = 1000$ ms, and the exponential decay (10) fits well (Fig. 1), from which we estimate a typical leakage time $\tau_{i\to e}$ of about 1700 ± 100 ms. Moreover the intracellular water fraction ρ_0 is equal to 0.42 ± 0.01, that yields $\tau_K = \tau_{i\to e}/\rho_0 = 4000 \pm 300$ ms. Note that the hypothesis $\delta \ll \tau_{i\to e}$ is valid.

The fast diffusion coefficient D_f does not depend on δ and slowly decreases with t_d, from 1.6 μm^2/ms at $t_d = 20.2$ ms to 1.2 μm^2/ms at $t_d = 1000$ ms (Fig. 1). As explained previously, one can interpret this decrease as the combined effect of hindered diffusion due to the high concentration of yeast cells and exchange with intracellular water. In [38] an asymptotic formula for the time dependent diffusion coefficient in a *dilute* suspension of

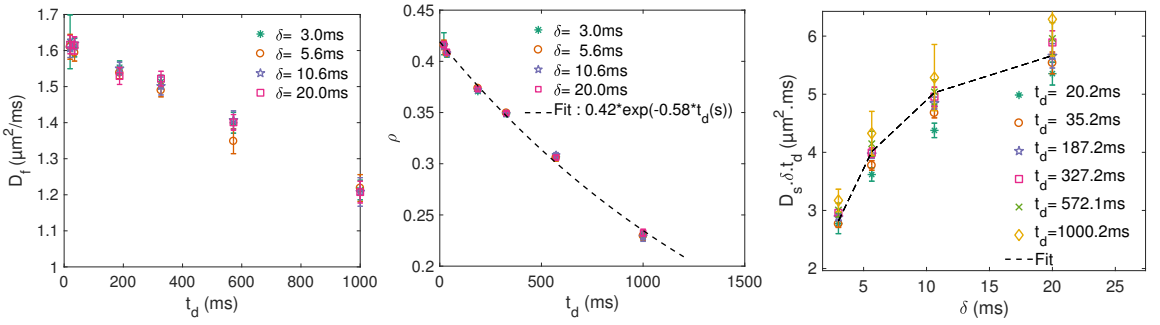

Fig. 1: Parameters obtained from the bi-exponential fit (6). (left) The fast ADC, D_f, as a function of the diffusion time t_d; (center) The intracellular water fraction ρ as a function of t_d. Dashed line shows an exponential fit (10), with $\rho_0 = 0.42$ and $\tau = 1700$ ms; (right) The product $D_s\delta t_d$ as a function of δ. Dashed line shows a fit of the curves by Eq. (4).

spheres was derived. This formula indicates that the diffusion coefficient decreases towards a limit value as t_d^{-1} with a typical time scale given by R^2/D_e, which in our case is equal to about 5 ms. In a *crowded* suspension one expects this time scale to be linked to some correlation length of the distribution of the cells. For example, if the cells aggregate and form clusters of size $L \gg R$, D_f will decrease with a time scale $L^2/D_e \gg R^2/D_e$. Numerous works have also been devoted to the infinite time limit of the diffusion coefficient outside an isotropic random suspension of spheres [56–60], with a common agreement on the upper bound:

$$\frac{D(t=\infty)}{D_e} \leq \frac{1-\rho}{1+\rho/2}\,, \tag{22}$$

where the exact value of $D(t=\infty)/D_e$ depends on the distribution of spheres. In particular, this upper bound is reached in the case of a "well-separated" array of spheres, that is a suspension with no aggregates. In our case, $\rho \approx 0.4$ so that Eq. (22) provides the upper bound $D(t=\infty)/D_e \leq 0.5$. The free diffusion coefficient of water at room temperature is around 2.3 μm^2/ms [61–63] thus the hindered diffusion coefficient should be lower than 1.2 μm^2/ms. However D_f is above 1.2 μm^2/ms even at t_d as high as 1000 ms. As a consequence, the exchange alone does not seem to explain the obtained values of D_f. Note that, in general, neglecting the effect of geometrical hindrance on the time variation of D_f leads to an underestimation of τ_K.

The product $D_s\delta t_d$ is not exactly constant but increases with δ (its value at $\delta = 20$ ms is approximately the double of its value at $\delta = 3$ ms) and slightly increases with t_d (a 20% increase from $t_d = 20$ ms to $t_d = 1000$ ms) (Fig. 1). The correction formula (4) accounts quite well for the variation with δ but is unable to reproduce the dependence on t_d because the correction term in Eq. (4) does not depend on t_d if $t_d \gg \delta$ (which is the case for almost all data points). We expect that the variation with t_d is caused by the exchange across the cell membranes. This dependence on t_d makes hard to give precise estimates of R and D_i. We get $R = 2.6 \pm 1$ μm and $D_i = 0.75 \pm 0.15$ μm^2/ms (95% confidence intervals), in agreement with the values found in the literature [55, 64].

4.2. Kärger model and modified Kärger model

On these experimental data, the Kärger model and the modified Kärger model yield very close values of the parameters, hence we only show in Fig. 2 a fit made with the modified Kärger model. In spite of small systematic deviations between the data and the model, the fit is good and yields (with 95% confidence intervals): $D_f = 1.73 \pm 0.03$ μm^2/ms, $D_i = 0.86 \pm 0.12$ μm^2/ms, $\rho = 0.413 \pm 0.002$, $\tau_K = 3700 \pm 100$ ms and $R = 2.7 \pm 0.07$ μm. From Eqs. (9) and (11) one deduces the permeability $\kappa = (5.8 \pm 0.4)\,10^{-4}$ μm/ms. These values are consistent with the literature [55, 64]. Figure 2 illustrates also the property that the low-q decay of the signal is independent of δ whereas the high-q decay is independent of t_d (more precisely, varying t_d changes only the amplitude but not the shape of the curve).

Note however that the Kärger model is only suited to fit data with several values of t_d and δ at the same time. If one tries to fit only one curve $S(q)$ (that is, with one value of t_d and one value of δ), the fit is unstable. Indeed, we have already noted that the bi-exponential model fits the data well (no sign of a systematic deviation, RMSE close to the noise level estimation). As a consequence, the addition of another parameter τ_K does not significantly improves the quality of the fit. Moreover, the fit algorithm returns very high values of τ_K associated with very large error bars. In turn, these large error bars on τ_K affect the stability of the whole fit because all the parameters are correlated (in particular ρ and τ_K). This can be understood by looking at Fig. 3. The signal is sensitive to τ_K only when $\tau_K \sim t_d$. As $\tau_K/t_d \to 0$ the

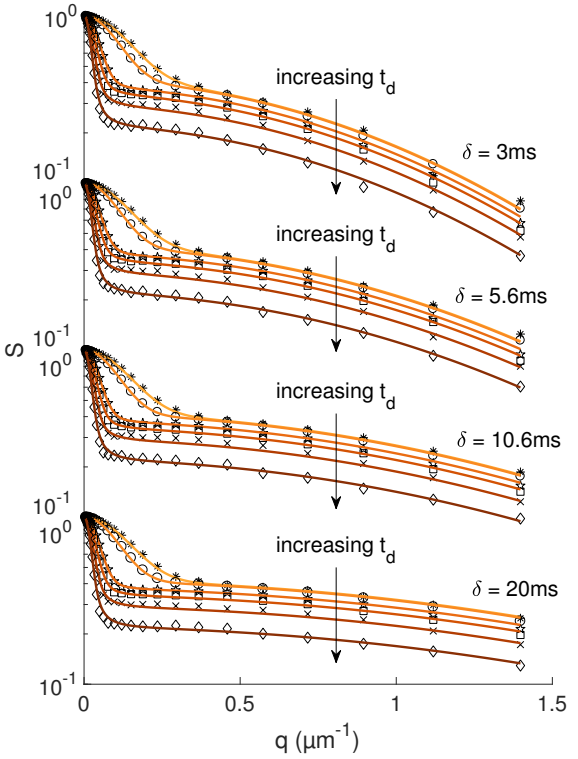

Fig. 2: Fit of the data by the modified Kärger model. The signal is plotted against $q = \gamma g \delta$ for various values of δ and t_d (asterisk: 20.2 ms, circle: 35.2 ms, star: 187.2 ms, square: 327.2 ms, cross: 572.1 ms, diamond: 1000.2 ms). Note that the plots are vertically shifted with different δ for visibility.

signal converges to the fast mono-exponential decay and as $\tau_K/t_d \to \infty$ the signal converges to the bi-exponential decay. As the bi-exponential fit is already good, the optimal value of τ_K is high compared to t_d and it is not well-determined. One also notices that the two curves with the highest τ_K (10^3 ms and 10^4 ms) have both the shape of a bi-exponential decay, the only difference being the apparent value of ρ (the amplitude of the slow high-q decay).

5. Conclusion

In summary, the bi-exponential model and both Kärger models yield rather close values of the parameters. In particular, the intracellular water fraction ρ and the exchange time τ_K are very similar. The bi-exponential model shows its limitations when it comes to the analysis of the slow apparent diffusion coefficient D_s. Indeed $D_s t_d$ weakly depends on t_d whereas it should not, according to Eq. (4). This effect may be attributed to the exchange. In the same way, the slow dependence of D_f on t_d may be caused by the exchange as well as by the

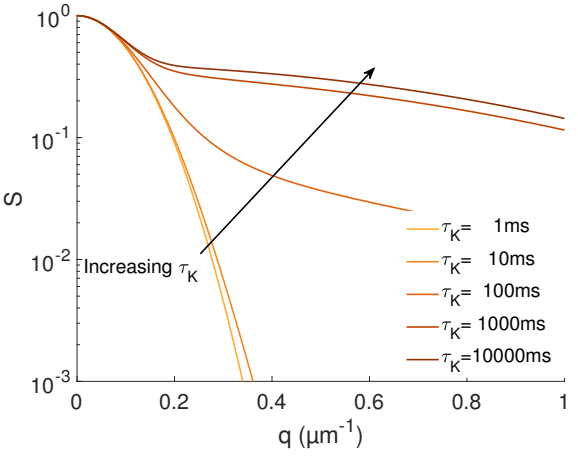

Fig. 3: The Kärger signal for $t_d = 100$ ms and various values of τ_K. While the signal increases with τ_K, the dependence on τ_K is weak when $\tau_K \ll t_d$ or $\tau_K \gg t_d$.

hindering by the cells. The errors bars on the parameters obtained from the bi-exponential model are also slightly larger than the ones obtained from the Kärger model.

The modified Kärger model is the most appropriate one from a theoretical point of view and can fit the whole data with one set of parameters. In some sense, this strength is also a weakness because the model is not applicable if one does not have full sets of data with variable q and t_d. Furthermore, this makes the model too "rigid"; for example, it is not clear how to take into account time-dependent diffusion coefficients.

On the other hand, the bi-exponential model with time-decaying ρ has a transparent physical interpretation and suggests the following experimental modality to quickly measure the exchange time: to choose a fixed value of q with fixed δ and to probe the signal as a function of diffusion time, for example with a multiple echo (CPMG) experiment (this is analogous to the Cg-simulations of Ref. [49]). At short times, the signal from the extracellular water is not completely destroyed, but at long times one only measures the intracellular signal, which decays as $\exp(-t/\tau_{i\to e})$, as shown above. Note that the same measurement without any weighting gradient is also needed in order to estimate the T_2-relaxation beforehand. This modality bears similarities with the FEXSY and FEXI sequences [65, 66] (where an additional filtering sequence is used to destroy the extracellular signal). From a theoretical point of view, one should choose δ large enough in order to be in the restricted diffusion regime but small compared to $\tau_{i\to e}$. This is only possible if $\tau_{i\to e} \gtrsim 50$ ms. Another condition is that the echo time TE should be chosen sufficiently long so that the extracellular magnetization is completely destroyed

between two echoes ($D_e q^2 TE \gg 1$) but still not too large compared to $\tau_{i\to e}$. On a conventional scanner with $g \leq 20$ mT/m these conditions require that $\tau_{i\to e} \gtrsim 250$ ms. With gradients higher than about 200 mT/m one can theoretically probe exchange time as short as 50 ms.

References

[1] P. T. Callaghan, Principles of Nuclear Magnetic Resonance Microscopy, 1st ed., Clarendon Press, 1991.

[2] W. Price, NMR Studies of Translational Motion: Principles and Applications, Cambridge Molecular Science, 2009.

[3] D. S. Grebenkov, NMR survey of reflected Brownian motion, Rev. Mod. Phys. 79 (2007) 1077–1137.

[4] D. S. Tuch, T. G. Reese, M. R. Wiegell, V. J. Wedeen, Diffusion MRI of complex neural architecture, Neuron 40 (2003) 885 – 895.

[5] J. Frahm, P. Dechent, J. Baudewig, K. Merboldt, Advances in functional MRI of the human brain, Prog. Nucl. Magn. Reson. Spectrosc. 44 (2004) 1 – 32.

[6] D. L. Bihan, H. Johansen-Berg, Diffusion MRI at 25: Exploring brain tissue structure and function, Neuroimage 61 (2012) 324 – 341.

[7] E. O. Stejskal, J. E. Tanner, Spin diffusion measurements: Spin echoes in the presence of a time-dependent field gradient, J. Chem. Phys. 42 (1965) 288–292.

[8] V. G. Kiselev, Fundamentals of diffusion MRI physics, NMR Biomed. 30 (2017) e3602.

[9] T. Niendorf, R. M. Dijkhuizen, D. G. Norris, M. van Lookeren Campagne, K. Nicolay, Biexponential diffusion attenuation in various states of brain tissue: Implications for diffusion-weighted imaging, Magn. Reson. Med. 36 (1996) 847–857.

[10] R. V. Mulkern, H. Gudbjartsson, C.-F. Westin, H. P. Zengingonul, W. Gartner, C. R. G. Guttmann, R. L. Robertson, W. Kyriakos, R. Schwartz, D. Holtzman, F. A. Jolesz, S. E. Maier, Multi-component apparent diffusion coefficients in human brain, NMR Biomed. 12 (1999) 51–62.

[11] C. A. Clark, D. Le Bihan, Water diffusion compartmentation and anisotropy at high b values in the human brain, Magn. Reson. Med. 44 (2000) 852–859.

[12] C.-L. Chin, F. W. Wehrli, S. N. Hwang, M. Takahashi, D. B. Hackney, Biexponential diffusion attenuation in the rat spinal cord: Computer simulations based on anatomic images of axonal architecture, Magn. Reson. Med. 47 (2002) 455–460.

[13] J. V. Sehy, J. J. Ackerman, J. J. Neil, Evidence that both fast and slow water ADC components arise from intracellular space, Magn. Reson. Med. 48 (2002) 765–770.

[14] Z. Ababneh, H. Beloeil, C. B. Berde, G. Gambarota, S. E. Maier, R. V. Mulkern, Biexponential parameterization of diffusion and T2 relaxation decay curves in a rat muscle edema model: Decay curve components and water compartments, Magn. Reson. Med. 54 (2005) 524–531.

[15] D. S. Grebenkov, Use, misuse, and abuse of apparent diffusion coefficients, Conc. Magn. Res. A 36A (2010) 24–35.

[16] A. Schwarcz, P. Bogner, P. Meric, J.-L. Correze, Z. Berente, J. Pl, F. Gallyas, T. Doczi, B. Gillet, J.-C. Beloeil, The existence of biexponential signal decay in magnetic resonance diffusion-weighted imaging appears to be independent of compartmentalization, Magn. Reson. Med. 51 (2004) 278–285.

[17] V. G. Kiselev, K. A. Il'yasov, Is the biexponential diffusion biexponential?, Magn. Reson. Med. 57 (2007) 464–469.

[18] G. J. Stanisz, Diffusion MR in biological systems: Tissue compartments and exchange, Isr. J. Chem. 43 (2003) 33–44.

[19] J.-H. Lee, C. S. Springer, Effects of equilibrium exchange on diffusion-weighted NMR signals: The diffusigraphic shutter-speed, Magn. Reson. Med. 49 (2003) 450–458.

[20] D. S. Novikov, V. G. Kiselev, Effective medium theory of a diffusion-weighted signal, NMR Biomed. 23 (2010) 682–697.

[21] J. Kärger, Zur Bestimmung der Diffusion in einem Zweibereich-system mit Hilfe von gepulsten Feldgradienten, Ann. Phys. 479 (1969) 1–4.

[22] J. Kärger, Der Einfluß der Zweibereichdiffusion auf die Spinechodämpfung unter Berücksichtigung der Relaxation bei Messungen mit der Methode der gepulsten Feldgradienten, Ann. Phys. 482 (1971) 107–109.

[23] J. Kärger, NMR self-diffusion studies in heterogeneous systems, Adv. Colloid Interface Sci. 23 (1985) 129 – 148.

[24] J. Kärger, H. Pfeifer, W. Heink, Principles and application of self-diffusion measurements by nuclear magnetic resonance, volume 12 of *Advances in Magnetic and Optical Resonance*, Academic Press, 1988, pp. 1 – 89. URL: `http://www.sciencedirect.com/science/article/pii/B9780120` doi:`10.1016/b978-0-12-025512-2.50004-x`.

[25] J.-P. Melchior, G. Majer, K.-D. Kreuer, Why do proton conducting polybenzimidazole phosphoric acid membranes perform well in high-temperature PEM fuel cells?, Physical Chemistry Chemical Physics 19 (2017) 601–612.

[26] A. Lauerer, R. Kurzhals, H. Toufar, D. Freude, J. Krger, Tracing compartment exchange by NMR diffusometry: Water in lithium-exchanged low-silica X zeolites, Journal of Magnetic Resonance 289 (2018) 1 – 11.

[27] E. Fieremans, D. S. Novikov, J. H. Jensen, J. A. Helpern, Monte Carlo study of a two-compartment exchange model of diffusion, NMR Biomed. 23 (2010) 711–724.

[28] M. Nilsson, D. van Westen, F. Ståhlberg, P. C. Sundgren, J. Lätt, The role of tissue microstructure and water exchange in biophysical modelling of diffusion in white matter, Magnetic Resonance Materials in Physics, Biology and Medicine 26 (2013) 345–370.

[29] J. Coatléven, H. Haddar, J.-R. Li, A macroscopic model including membrane exchange for diffusion MRI, SIAM J. Appl. Math. 74 (2014) 516–546.

[30] J.-R. Li, H. T. Nguyen, D. V. Nguyen, H. Haddar, J. Coatléven, D. L. Bihan, Numerical study of a macroscopic finite pulse model of the diffusion MRI signal, J. Magn. Reson. 248 (2014) 54 – 65.

[31] W. S. Price, A. V. Barzykin, K. Hayamizu, M. Tachiya, A model for diffusive transport through a spherical interface probed by pulsed-field gradient NMR, Biophys. J. 74 (1998) 2259 – 2271.

[32] C. H. Neuman, Spin echo of spins diffusing in a bounded medium, J. Chem. Phys. 60 (1974) 4508–4511.

[33] B. Robertson, Spin-echo decay of spins diffusing in a bounded region, Phys. Rev. 151 (1966) 273–277.

[34] T. M. de Swiet, P. N. Sen, Decay of nuclear magnetization by bounded diffusion in a constant field gradient, J. Chem. Phys. 100 (1994) 5597–5604.

[35] M. D. Hurlimann, K. G. Helmer, T. M. Deswiet, P. N. Sen, C. H. Sotak, Spin echoes in a constant gradient and in the presence of simple restriction, Journal of Magnetic Resonance, Series A 113 (1995) 260 – 264.

[36] D. S. Grebenkov, Exploring diffusion across permeable barriers at high gradients. II. Localization regime, J. Magn. Reson. 248 (2014) 164–176.

[37] V. G. Kiselev, D. S. Novikov, Transverse NMR relaxation in biological tissues, NeuroImage (2018).

[38] T. M. de Swiet, P. N. Sen, Time dependent diffusion coefficient in a disordered medium, J. Chem. Phys. 104 (1996) 206–209.

[39] P. N. Sen, Time-dependent diffusion coefficient as a probe of geometry, Conc. Magn. Res. A 23A (2004) 1–21.

[40] D. S. Novikov, J. H. Jensen, J. A. Helpern, E. Fieremans, Revealing mesoscopic structural universality with diffusion, PNAS 111 (2014) 5088–5093.

[41] S. D. Stoller, W. Happer, F. J. Dyson, Transverse spin relaxation in inhomogeneous magnetic fields, Phys. Rev. A 44 (1991) 7459–7477.
[42] P. T. Callaghan, A. Coy, D. MacGowan, K. J. Packer, F. O. Zelaya, Diffraction-like effects in NMR diffusion studies of fluids in porous solids, Nature 351 (1991) 467–469.
[43] B. Sapoval, General formulation of laplacian transfer across irregular surfaces, Phys. Rev. Lett. 73 (1994) 3314–3316.
[44] B. Sapoval, M. Filoche, E. R. Weibel, Smaller is better—but not too small: A physical scale for the design of the mammalian pulmonary acinus, PNAS 99 (2002) 10411–10416.
[45] D. S. Grebenkov, Scaling properties of the spread harmonic measures, Fractals 14 (2006) 231–243.
[46] D. Grebenkov, Partially Reflected Brownian Motion: A Stochastic Approach to Transport Phenomena, Nova Science Publishers, 2006, pp. 135–169. URL: https://www.novapublishers.com/catalog/product_info.php?products_id=3636.
[47] H. T. Nguyen, D. Grebenkov, D. V. Nguyen, C. Poupon, D. L. Bihan, J.-R. Li, Parameter estimation using macroscopic diffusion MRI signal models, Physics in Medicine & Biology 60 (2015) 3389.
[48] L. Ning, M. Nilsson, S. Lasič, C.-F. Westin, Y. Rathi, Cumulant expansions for measuring water exchange using diffusion MRI, J. Chem. Phys. 148 (2018) 074109.
[49] C. Meier, W. Dreher, D. Leibfritz, Diffusion in compartmental systems. I. A comparison of an analytical model with simulations, Magn. Reson. Med. 50 (2003) 500–509.
[50] J. E. Tanner, Use of the stimulated echo in NMR diffusion studies, J. Chem. Phys. 52 (1970) 2523–2526.
[51] I. Åslund, C. Cabaleiro-Lago, O. Söderman, D. Topgaard, Diffusion NMR for determining the homogeneous length-scale in lamellar phases, J. Phys. Chem. B 112 (2008) 2782–2794. PMID: 18271569.
[52] I. Åslund, B. Medronho, D. Topgaard, O. Söderman, C. Schmidt, Homogeneous length scale of shear-induced multilamellar vesicles studied by diffusion NMR, J. Magn. Reson. 209 (2011) 291 – 299.
[53] S. Lasič, I. Åslund, C. Oppel, D. Topgaard, O. Söderman, M. Gradzielski, Investigations of vesicle gels by pulsed and modulated gradient NMR diffusion techniques, Soft Matter 7 (2011) 3947–3955.
[54] S. Eriksson, K. Elbing, O. Söderman, K. Lindkvist-Petersson, D. Topgaard, S. Lasič, NMR quantification of diffusional exchange in cell suspensions with relaxation rate differences between intra and extracellular compartments, PLoS One 12 (2017) 1–18.
[55] I. Åslund, D. Topgaard, Determination of the self-diffusion coefficient of intracellular water using PGSE NMR with variable gradient pulse length, J. Magn. Reson. 201 (2009) 250 – 254.
[56] J. C. Maxwell, A treaty on eletricity and magnetism, volume 1, 2nd ed., Clarendon Press, 1873.
[57] Z. Hashin, S. Shtrikman, A variational approach to the theory of the effective magnetic permeability of multiphase materials, J. Appl. Phys. 33 (1962) 3125–3131.
[58] H. L. Weissberg, Effective diffusion coefficient in porous media, J. Appl. Phys. 34 (1963) 2636–2639.
[59] D. J. Jeffrey, Conduction through a random suspension of spheres, Proc. Roy. Soc. Lond. A 335 (1973) 355–367.
[60] J. van Brakel, P. Heertjes, Analysis of diffusion in macroporous media in terms of a porosity, a tortuosity and a constrictivity factor, Int. J. Heat Mass Transfer 17 (1974) 1093–1103.
[61] P. Tofts, D. Lloyd, C. Clark, G. Barker, G. Parker, P. McConville, C. Baldock, J. Pope, Test liquids for quantitative MRI measurements of self-diffusion coefficient in vivo, Magn. Reson. Med. 43 (2000) 368–374.
[62] R. Mills, Self-diffusion in normal and heavy water in the range 1-45, J. Phys. Chem. 77 (1973) 685–688.
[63] J. H. Wang, Self-diffusion coefficients of water, J. Phys. Chem. 69 (1965) 4412–4412.
[64] D. S. Grebenkov, D. V. Nguyen, J.-R. Li, Exploring diffusion across permeable barriers at high gradients. I. Narrow pulse approximation, J. Magn. Reson. 248 (2014) 153–163.
[65] I. Åslund, A. Nowacka, M. Nilsson, D. Topgaard, Filter-exchange PGSE NMR determination of cell membrane permeability, J. Magn. Reson. 200 (2009) 291 – 295.
[66] S. Lasič, M. Nilsson, J. Lätt, F. Ståhlberg, D. Topgaard, Apparent exchange rate mapping with diffusion MRI, Magn. Reson. Med. 66 (2011) 356–365.